XRF analysis by the fusion method for oxide powder on a benchtop WDXRF spectrometer Supermini

Yasujiro Yamada*

1. Introduction

The fusion method in X-ray fluorescence (XRF) analysis is an effective sample preparation technique for getting accurate analysis results of powder samples, since the technique eliminates heterogeneity due to grain size and mineralogical effect. In addition, the homogenization of material property by vitrification makes it possible to expand the calibration range, such as making synthetic calibration curves by the use of reagents or applying the calibration to diverse materials.

A benchtop wavelength-dispersive X-ray fluorescence (WDXRF) spectrometer Supermini is compact and yet has excellent resolution and sensitivity for light elements. This report demonstrates that single calibration for diverse minerals and ores was established by the fusion method on the Supermini.

2. Problems and solutions of the fusion method applied to diverse materials

XRF is an analysis method using calibration curves prepared with standard samples for each kind of material to be analyzed. For the analysis of various minerals and ores, however, the number of standard samples available in the market for every kind of material is limited.

Meanwhile, the best fusion condition for making fusion beads is different for each kind of material. For example, a typical dilution ratio of sample to flux in weight is 10 : 1, but in the case of samples containing high transition metals, it should be a higher dilution ratio 20 : 1 to make proper fusion beads. In addition, chrome-magnesia refractory samples require additional oxidizing agent during the fusion.

Crystallization water, carbonate and so on may cause loss on ignition (LOI) due to evaporation of H_2O or CO_2 during the fusion. On the other hand, there is a case of gain on ignition (GOI), such as iron ore, due to oxidization of the component.

In the case of analysis for diverse materials, there is another problem where the difference in major elements among variety of sample materials causes the difference of absorption and enhancement effect to fluorescent X-rays emitted from the samples. This effect results in analysis error.

The problems stated above are summarized as following three factors causing analysis error,

(1) Difference in dilution ratio of flux and oxidizing agent to sample
(2) LOI and GOI
(3) Matrix effect.

For (1), it is possible to apply correction for dilution ratio of the flux to the sample and, if necessary, additional correction for weight ratio of oxidizing agent component left in the bead to the sample. About oxidizing agent (*e.g.* $LiNO_3$), a part of the agent (*e.g.* NO_2) is evaporated during the fusion and the rest (*e.g.* Li_2O) is left in the bead. The correction coefficients can be calculated by the use of the fundamental parameter method (hereafter FP method).

For (2), it is possible to compensate for the influence of LOI and GOI by treating LOI and GOI as non-measured component (balance component) in the matrix correction formula.

For (3), it is necessary to apply the proper matrix correction model as in the conventional way, where the correction coefficients can be obtained by the FP method.

The solutions for the problems (1), (2) and (3) have been already reported[(1)–(3)]. The correction formula will be described below.

The dilution ratios of the flux to the sample R_F and the weight ratio of the oxidizing agent component left in the bead to the sample (hereafter oxidizer ratio) R_X are expressed as follows,

$$R_F = \overline{R}_F + \Delta R_F \quad (1)$$

$$R_X = \overline{R}_X + \Delta R_X \quad (2)$$

where $\overline{R}_F$ is the standard dilution ratio, $\overline{R}_X$ the standard oxidizer ratio, ΔR_F the difference between the dilution ratio and the standard dilution ratio, and ΔR_X the difference between the oxidizer ratio and the standard dilution ratio.

The calibration equation with correction terms of dilution ratio and oxidizer ratio is expressed as follows,

$$C_i = (A_i I_i + B_i)\left(1 + \sum_j \alpha_j C_j + \alpha_F \Delta R_F + \alpha_X \Delta R_X\right) \quad (3)$$

C_i : weight fraction of the analyte in the sample
C_j : weight fraction of the coexisting component in the sample
A_i, B_i : calibration constants
α_j : matrix correction coefficient for component j
α_F : matrix correction coefficient for the flux

* SBU WDX, X-ray Analysis Division, Rigaku Corporation.

α_X : matrix correction coefficient for the oxidizing agent component left in the bead.

Substituting the equations (1) and (2) into the equation (3), the following equation is obtained,

$$C_i = (A_i I_i + B_i)\left(1 + \sum_j \alpha_j C_j + K_i + \alpha_F R_F + \alpha_X R_X\right) \quad (4)$$

where $K_i = -(\alpha_F \bar{R}_F + \alpha_X \bar{R}_X)$.

Since K_i is a constant, it is possible to use the actual weights for the flux, sample and oxdizing agent for the dilution ratio and the oxidizer ratio, which results in accurate corrections for the described losses and gains.

The correction coefficient α_j, α_F and α_X are calculated by the use of the FP method, where the effect of LOI and GOI is compensated by applying the correction model in which the balance component is designated as the base component.

3. Expansion of analysis range by the use of reagents in the fusion method

Standard samples commercially available are quite limited as mentioned above. One of the features of the fusion method is that the standard samples for calibration can be made with synthetic oxides.

When making synthetic standard beads by the use of reagents, typically two or more reagents are mixed to make a fusion bead. In the analysis of this report, however, to simplify the procedure, a single reagent was used to make a fusion bead for expanding the quantitation range for each analyte. The analytes, the reagents used and the procedure for expanding the calibration range are shown below.

[Na_2O]

Sodium carbonate (Na_2CO_3) was dried at 230℃, weighed out so that the residual Na_2O become 25 mass% in the fusion bead with the dilution ratio 10 : 1 and then fused. The balance was 75%, treated as LOI.

[Al_2O_3]

Alumina (Al_2O_3) was baked at 1050℃, weighed out so that Al_2O_3 become 100 mass% in the fusion bead with the dilution ratio 10 : 1 and then fused.

[P_2O_5]

Lithium Phosphate (Li_3PO_4) was dried at 700℃, weighed out so that the residual P_2O_5 become 25 mass% in the fusion bead with the dilution ratio 10 : 1 and then fused.

[K_2O]

Potassium Carbonate (K_2CO_3) was dried at 230℃, weighed out so that the residual K_2O become 50 mass% in the fusion bead with the dilution ratio 10 : 1 and then fused.

[CaO]

Calcium Carbonate ($CaCO_3$) was dried at 230℃, weighed out so that the residual CaO become 100 mass% in the fusion bead with the dilution ration 10 : 1 and then fused. The expanded calibration covers quick lime.

[TiO_2]

Titanium Oxide (TiO_2) was dried at 1000℃, weighed out so that the TiO_2 become 10 mass% in the fusion bead with the dilution ratio 10 : 1 and then fused.

Table 1. Standard materials used in this analysis.

BAS	
Number	Material
BAS203a	Talc
BCS313-1	High purity silica
BCS314	Silica brick
BCS315	Fire brick
BCS368	Dolomite
BCS369	Magnesite chrome (Chrome-magnesia)
BCS370	Magnesite chrome (Chrome-magnesia)
BCS375	Soda feldspar
BCS376	Potash feldspar
BCS358	Zirconia
BCS389	High purity magnesia
BCS393	Limestone
BCS394	Calcined Bauxite
BCS395	Bauxite
BAS 683	Iron Ore

NIST	
Number	Material
NBS98a	Plastic Clay
NBS120c	Florida Phosphate Rock
SRM 1c	Argillaceous Limestone
SRM 69b	Bauxite (Arkansas)
SRM 696	Bauxite, Surinam
SRM 697	Bauxite, Dominican
SRM 698	Bauxite, Jamaican
SRM 70a	Feldspar, Potash
SRM 99a	Feldspar, Soda
NIST81a	Glass Sand
NIST1413	Glass Sand (High Alumina)
NBS694	Phosphate Rock, Western

CSJ	
Number	Material
R-603	Clay
R-701	Feldspar
R-801	Agalmatolite

TARJ	
Number	Material
JRRM511	Chrom-magnesia refractory
JRRM602	Zircon-zirconia refractory
JRRM701	Alumina-zircon-silica refractory

JCA	
Number	Material
RM-611	Portland cement
RM-612	Portland cement
RM-613	Portland cement

ECISS	
Number	Material
ECISS782	Dolomite
ECISS776	Fire Brick

JSS	
Number	Material
JSS009-2	Pure iron oxide (III)

Table 2. Concentration range of the standard samples and calibration range.

(unit: mass%)

Component	Conc. range of reference materials	Calibration range	Component	Conc. range of reference materials	Calibration range
Na_2O	0.003 – 10.4	0.003 – 25.0	MnO	0.000 – 0.596	0.000 – 0.596
MgO	0.001 – 96.7	0.001 – 96.7	Fe_2O_3	0.012 – 99.84	0.012 – 99.84
Al_2O_3	0.036 – 88.8	0.036 – 100	Cr_2O_3	0.001 – 52.51	0.001 – 52.51
SiO_2	0.2 – 99.78	0.2 – 99.78	ZrO_2	0.034 – 92.7	0.034 – 92.7
P_2O_5	0.004 – 33.34	0.004 – 33.34	HfO_2	0.00 – 1.63	0.00 – 1.63
K_2O	0.004 – 11.8	0.004 – 50.0	SO_3	0.001 – 6.07	0.001 – 6.07
CaO	0.006 – 66.25	0.006 – 100	SrO	0.003 – 0.28	0.003 – 0.28
TiO_2	0.004 – 4.961	0.004 – 10.0	LOI	0.00 – 47.4	0.00 – 90

Note: number with underline means the concentration of the synthetic standard samples.

Table 3. Measurement condition.

Component	Na_2O	MgO	Al_2O_3	SiO_2	P_2O_5	SO_3	K_2O	CaO
Element line	Na-Kα	Mg-Kα	Al-Kα	Si-Kα	P-Kα	S-Kα	K-Kα	Ca-Kα
Primary beam filter	Out	Out	Out	Out	Out	Out	Al	Out
Analyzing crystal	RX25	RX25	PET	PET	PET	PET	PET	PET
Detector	F-PC	F-PC	F-PC	F-PC	F-PC	F-PC	F-PC	F-PC
Counting time Peak (sec)	20	20	20	20	20	20	20	20
BG (sec)	20	20	20	20	20	20	20	20
Component	TiO_2	Cr_2O_3	MnO	Fe_2O_3	SrO	ZrO_2	HfO_2	
Element line	Ti-Kα	Cr-Kα	Mn-Kα	Fe-Kα	Sr-Kα	Zr-Lα	Hf-Lβ1	
Primary beam filter	Out	Out	Out	Out	Out	Out	Out	
Analyzing crystal	LiF(200)	LiF(200)	LiF(200)	LiF(200)	LiF(200)	PET	LiF(200)	
Detector	SC	SC	SC	SC	SC	F-PC	SC	
Counting time Peak (sec)	20	20	20	20	20	20	20	
BG (sec)	20	20	20	20	20	20	20	

4. Standard materials and calibration range

Table 1 shows the standard reference materials used in this analysis. Thirty nine standard materials of talc, high purity silica, feldspar, dolomite, bauxite, iron ore, cement, phosphate rock and others were used. Table 2 shows the concentration range of the standard materials used and also the calibration range including synthetic oxide standard samples mentioned above. The range for MgO, Al_2O_3, SiO_2, Fe_2O_3, ZrO_2, etc. is from a trace to 90 mass% or higher and the range for P_2O_5 CaO, Cr_2O_3 is 30−60 mass%. In addition, the calibration is applicable to samples with up to 50 mass% LOI.

5. Sample preparation

In the fusion, lithium tetra borate ($Li_2B_4O_7$), pre-dried at 675℃, was used as flux and lithium nitrate ($LiNO_3$) as oxidizing agent. The dilution ratio of the flux to the sample in weight was 20 : 1 only for magnesite chrome and chrome-magnesia refractory and 10 : 1 for the others.

The oxidizing agent $LiNO_3$ was used only for chrome-magnesia refractory and the weight ratio of $LiNO_3$ to the sample was 10 : 1. $LiNO_3$ is evaporated during the fusion by the following reaction,

$$2LiNO_3 \rightarrow Li_2O + 5/2O_2\uparrow + N_2\uparrow$$

and, therefore, the residual component of the oxidizing agent left in the fusion bead is Li_2O. Accordingly, the weight ratio of the residual component to the sample ("oxidizer ratio" mentioned earlier in Clause 2) is 2.1668.

The samples were fused on Rigaku benchtop high-frequency fusion machine, Bead Sampler. The fusion temperature was 1200℃ for all materials except for Portland cement, which was fused at 1075℃ to prevent volatilization of sulfur, one of the analytes.

6. Instrument and measurement condition

Each fusion bead was measured in vacuum on the Supermini, a benchtop WDXRF spectrometer, which was equipped with an end-window Pd-target 200 W X-ray tube, operating at 50 kV−4.0 mA, with the measurement area 30 mm in diameter. Details of the measurement conditions are shown in Table 3. The measurement time for the analysis of the 15 components per sample was about 12 minutes.

7. Calibration and analysis results

The calibration results are summarized in Table 4 and the calibration curves are shown in Figs. 1−15.

With respect to matrix correction, since samples containing a large amount of LOI were fused to make fusion beads, the de Jongh model in which all analytes were correcting components was applied to calculate theoretical matrix correction coefficients. LOI (and GOI) was designated as the balance and the base component to compensate for the influence of LOI (and GOI)

Table 4. Calibration range and accuracy.

Component	Calibration Range (mass%)	Accuracy (mass%)	Fig.
SiO_2	0.2 – 99.78	0.27	1
Al_2O_3	0.036 – 100	0.26	2
MgO	0.001 – 96.7	0.18	3
Na_2O	0.003 – 25.0	0.075	4
CaO	0.006 – 100	0.30	5
K_2O	0.004 – 50.0	0.032	6
P_2O_5	0.004 – 33.34	0.049	7
TiO_2	0.004 – 10.0	0.043	8
MnO	0.000 – 0.596	0.067	9
Fe_2O_3	0.012 – 99.84	0.26	10
Cr_2O_3	0.001 – 52.51	0.038	11
ZrO_2	0.034 – 92.7	0.34	12
HfO_2	0.00 – 1.63	0.035	13
SO_3	0.001 – 6.07	0.031	14
SrO	0.003 – 0.28	0.003	15

though LOI (or GOI) content is unknown.

Even though various standard materials and additional synthetic standards were used for making the calibration curves, excellent accuracy was obtained for each and all of the analytes.

When an element line of an analyte is interfered with by other element lines, it is necessary to apply appropriate overlap correction. In this analysis, correction for overlap of Zr–Lα to P–Kα, of Cr–Kβ1 to Mn–Kα, of P–Kα to Zr–Lα and Zr–Lγ1 on S–Kα was carried out.

For the typical analytes, the details are explained.

[SiO_2]

Figure 1 shows the calibration curve of SiO_2. Excellent accuracy 0.27 mass% was obtained though the calibration range was expanded from 0 to almost 100 mass% by including high purity silica as a standard sample. The typical materials are shown in the figures.

Although LOI-rich limestone and dolomite, and chrome-magnesia with the different dilution ratio are included, the calibration curve shows a good fit with appropriate correction applied.

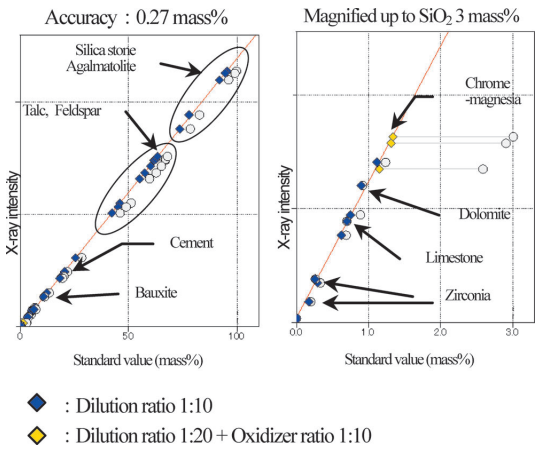

Fig. 1. SiO_2 calibration curve.

[Al_2O_3]

Figure 2 shows the calibration curve of Al_2O_3. In spite of the wide calibration range from 0 to 100 mass% by including Al_2O_3 synthetic bead, excellent accuracy 0.26 mass% was obtained.

The plot of the synthetic Al_2O_3 bead is right on the line by regression with the reference materials. Regardless of variation of LOI content and dilution ratio with wide variation of the standard samples, the calibration curve shows a good fitting.

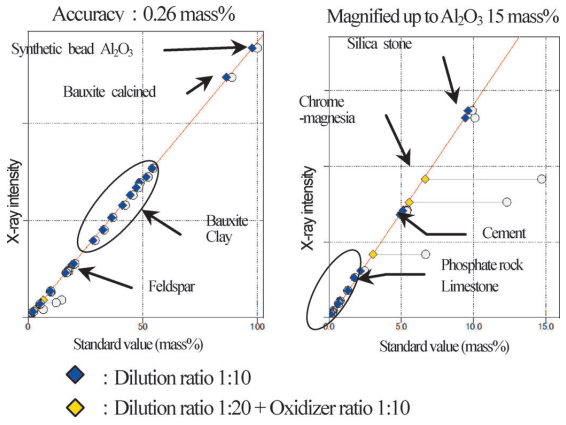

Fig. 2. Al_2O_3 calibration curve.

[MgO]

Figure 3 shows the calibration curve of MgO. Excellent accuracy 0.18 mass% was obtained for calibration range up to ~97 mass% of high purity magnesia. In spite of a lack of standards between 50–90 mass%, the calibration curve shows a good linearity from low concentration to high concetnration, which means that it is possible to quantify MgO content through this calibration range.

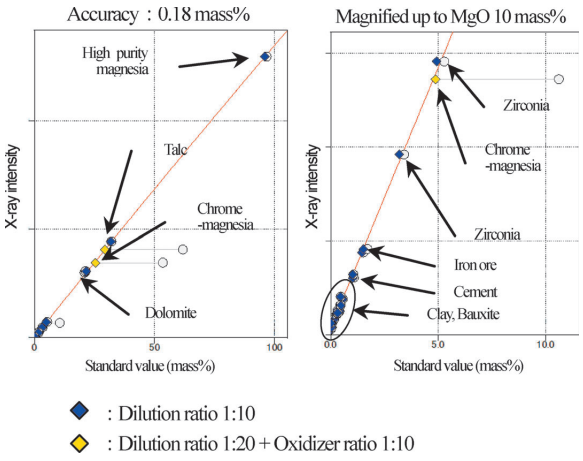

Fig. 3. MgO calibration curve.

[Na_2O]

Figure 4 shows the calibration curve of Na_2O. The Na_2O 25 mass% synthetic bead out of sodium carbonate agent (indicated as Na_2O 25) is plotted right on the regression line with the standard materials, which

demonstrated that a calibration range can be extended easily by the use of a single component agent to make a synthetic standard bead. In addtion, the calibration curve shows an excellent linearity with wide variation of the materials.

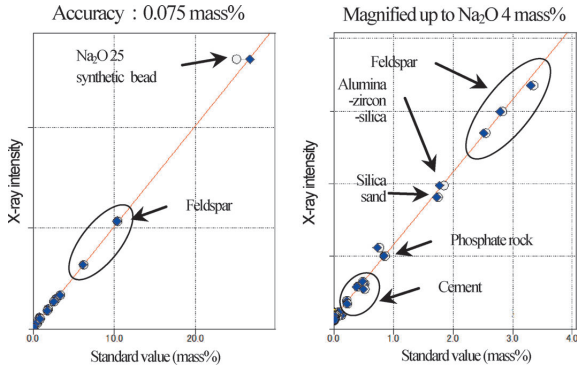

Fig. 4. Na_2O calibration line.

[CaO]

Figure 5 shows the calibration curve of CaO, which includes the fusion bead made with $CaCO_3$ agent at the dilution ratio 10 : 1 as the component CaO is 100 mass% (indicated as CaO 100). In spite of wide varaity of the material and LOI content, the calibration curve shows a good linearity up to 100 mass%.

8. Summary

This report demonstrated that the fusion method and the corrections for LOI/GOI and the dilution ratio of flux and oxidizing agent enable a single calibration with the wide range of concentration and for diverse natural minerals and ores. In addition, it was also shown that it is possible to extend the calibration range by the use of a single agent to make a synthetic standard fusion bead.

The Supermini is a benchtop WDXRF spectrometer equipped with an air-cooled 200 W X-ray tube to deliver excellent sensitivity and resolution from light elements to heavy elements while eliminating typical installation requirements, such as cooling water, special power supply and large floor space. Therefore, this model can be used for analysis of wide variety of natural minerals and ores under various environments.

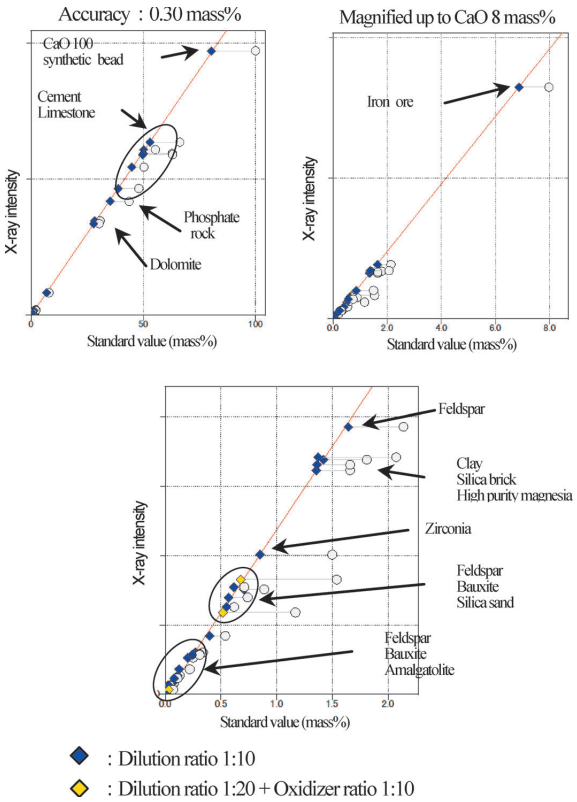

Fig. 5. CaO calibration curve.

References

(1) Y. Kataoka, S. Shoji and H. Kohno: *Advances in X-Ray Chemical Analysis, Japan*, **23** (1992), 171−175.

(2) S. Shoji, K. Yamada, E. Furusawa, H. Kohno and M. Murata: *Advances in X-Ray Chemical Analysis, Japan*, **23** (1992), 177−187.

(3) Rigaku Application Note XRF5027, Determination of Metals in Copper Concentrate by Advanced Correction Method for Fused Beads.

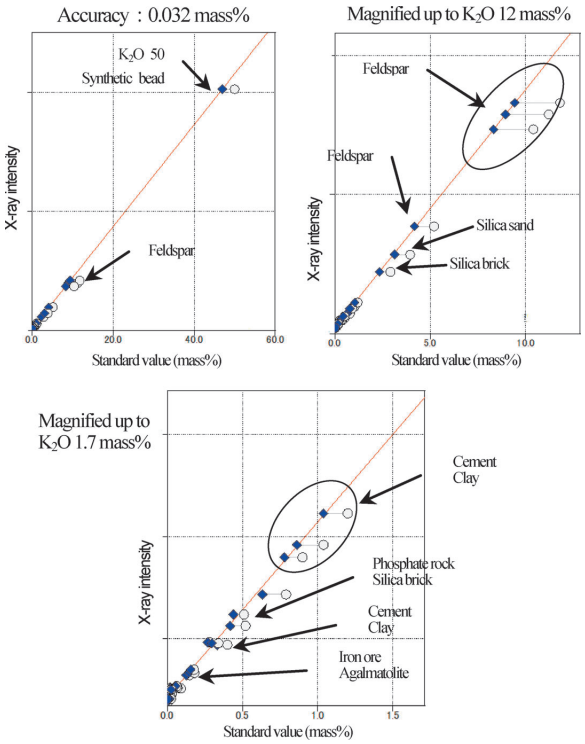

Fig. 6. K_2O calibration curve.

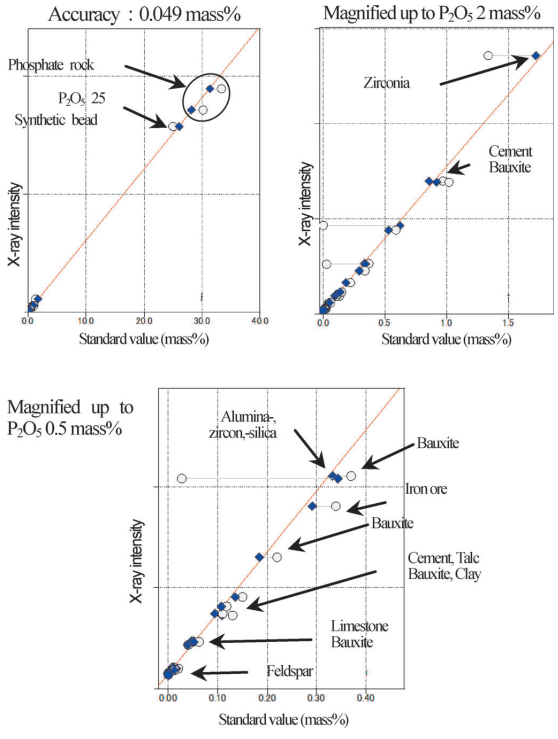

Fig. 7. P_2O_5 calibration curve.

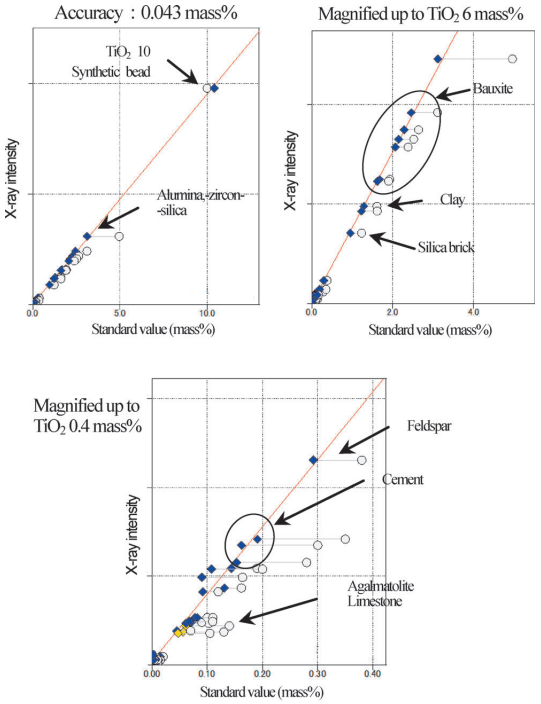

Fig. 8. TiO_2 calibration curve.

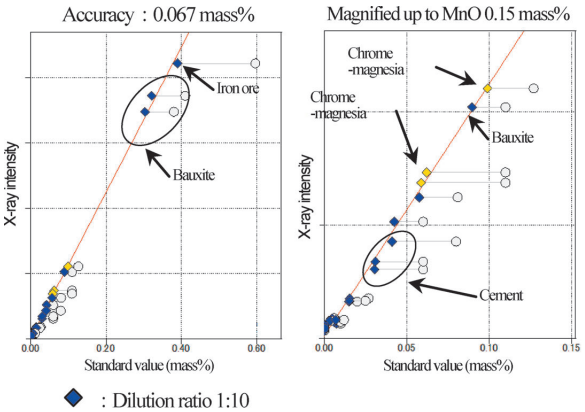

Fig. 9. MnO calibration curve.

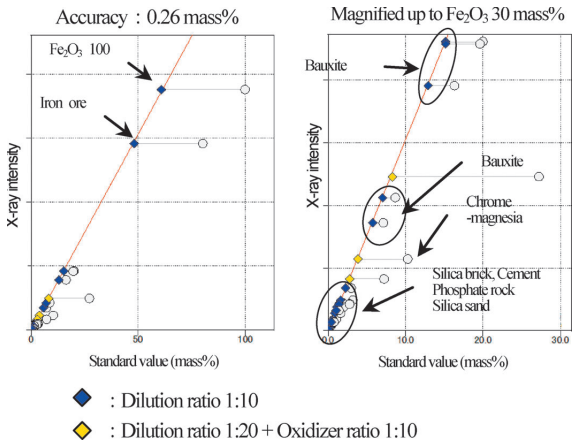

Fig. 10. Fe_2O_3 calibration curve.

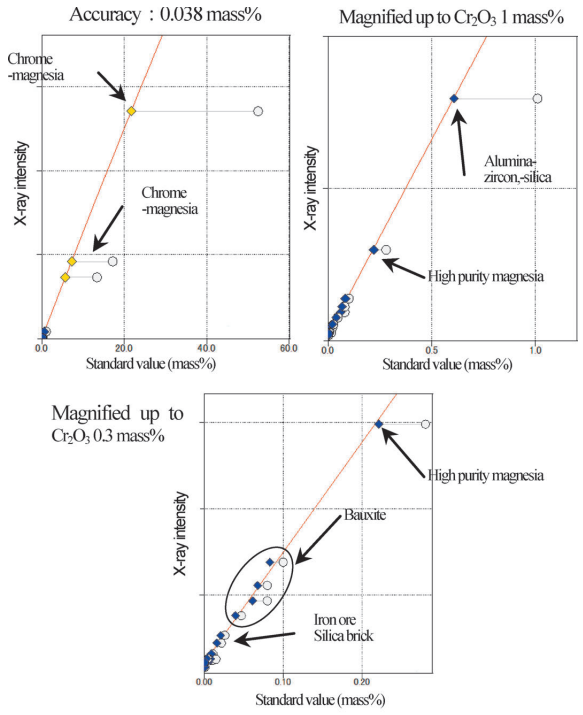

Fig. 11. Cr_2O_3 calibration curve.

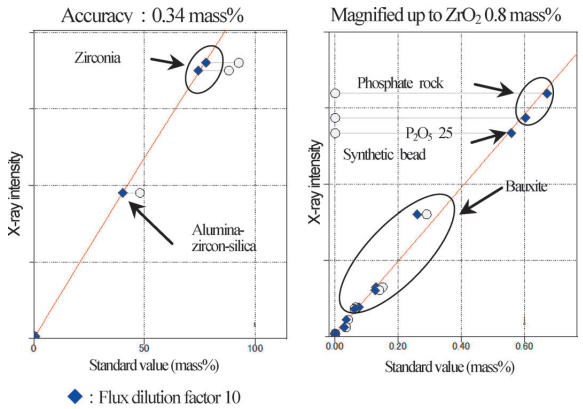

Fig. 12. ZrO_2 calibration curve.

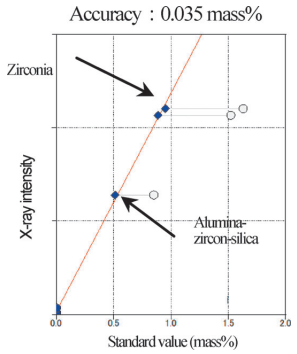

Fig. 13. HfO_2 calibration curve.

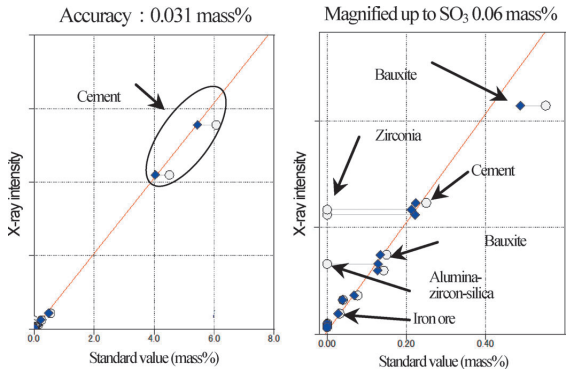

Fig. 14. SO_3 calibration curve.

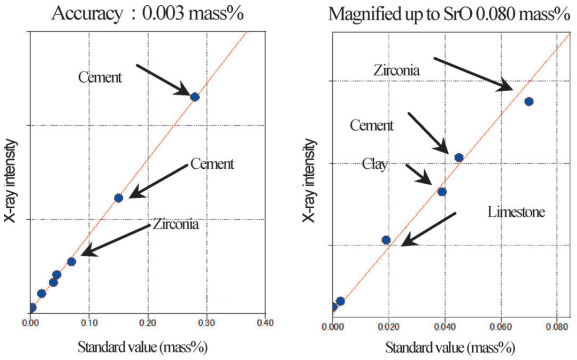

Fig. 15. SrO calibration curve.
Since the Sr-Kα line is affected by the thickness of fusion bead due to its high energy, correction for thickness and matrix effect by internal standard method was applied with intensity ratio of Sr-Kα and its background.